

This article appeared in a journal published by Elsevier. The attached copy is furnished to the author for internal non-commercial research and education use, including for instruction at the authors institution and sharing with colleagues.

Other uses, including reproduction and distribution, or selling or licensing copies, or posting to personal, institutional or third party websites are prohibited.

In most cases authors are permitted to post their version of the article (e.g. in Word or Tex form) to their personal website or institutional repository. Authors requiring further information regarding Elsevier's archiving and manuscript policies are encouraged to visit:

<http://www.elsevier.com/copyright>



Contents lists available at SciVerse ScienceDirect

Journal of Virological Methods

journal homepage: www.elsevier.com/locate/jviromet

Characterization of isolates of *Citrus tristeza virus* by sequential analyses of enzyme immunoassays and capillary electrophoresis-single-strand conformation polymorphisms

G. Licciardello^{a,*}, D. Raspagliesi^a, M. Bar-Joseph^b, A. Catara^a^a Laboratory for Phytosanitary Diagnoses and Biotechnology, Science and Technology Park of Sicily s.c.p.a., Blocco Palma I, Z.I. 95121 Catania, Italy^b Gimlaotec, 8 Hazananim St., Rehovot 76211, Israel

A B S T R A C T

Article history:

Received 6 October 2011

Accepted 17 January 2012

Available online 26 January 2012

Keywords:

CTV

Single strands conformation analysis

Citrus

Capillary electrophoresis

Immunoassay

Typing

Citrus tristeza virus (CTV) is the causal agent of tristeza disease, which is one of the most devastating diseases of citrus crops worldwide. This paper describes a method for the rapid detection and genotyping of naturally spreading CTV isolates. This method uses ELISA or dot-blot immunological tests to detect trees infected with CTV. The reaction wells or membrane spots for which there is a positive reaction are sequentially treated by (i) washing and elution of viral RNA from the trapped samples, (ii) one-step synthesis of cDNA and PCR and (iii) automated fluorescence-based capillary electrophoresis single-strand conformation polymorphism (CE-SSCP) analysis of amplification products. Comparative CE-SSCP results are presented for CTV RNA extracted directly from infected leaves and ELISA plates or from membranes. In the analyses of all of these RNA samples, the p18, p27 and p23 CTV genes were targeted for amplification.

Specific profiles of forward and reverse strands were obtained from a group of eight CTV isolates collected in Sicily, each with distinct biological characteristics, which were analyzed using the conventional two-step procedure (immunological detection followed by CE-SSCP molecular characterization after RNA isolation) or in a continuous process of ELISA/CE-SSCP or dot-blot/CE-SSCP starting from infected plant material. The combined method is simple, highly sensitive and reproducible, thus allowing the processing of numerous field samples for a variety of epidemiological needs. The sequential processing of an ELISA or dot-blot/ELISA followed by CE-SSCP is expected to allow the rapid detection of recent CTV infections along with the simultaneous characterization of the genetic diversity and structure of the population of newly invading CTV.

© 2012 Elsevier B.V. All rights reserved.

1. Introduction

Citrus tristeza virus (CTV) is the causal agent of tristeza disease, which is considered to be one of the most devastating diseases of citrus crops (Bar-Joseph et al., 1989; Karasev and Hilf, 2010; Moreno et al., 2008). CTV is the largest known plant RNA virus. It consists of a single positive strand of genomic RNA that is about 19.3 kb in length (Bar-Joseph and Dawson, 2008; Dawson, 2010; Karasev et al., 1995). Its two ends are encapsidated by different coat proteins, a major coat protein (CP) of 25 kDa and a minor coat protein (CPm) of 27 kDa. The CP encapsidates the main part of the virion and the CPm encapsidates about 3% of the 5' end of the genomic RNA (Febres et al., 1996). About 20 CTV genomes have been fully sequenced from isolates collected in different geographic regions (Albiach-Martí et al., 2000; Harper et al., 2010; Karasev et al., 1995;

Mawassi et al., 1996; Ruiz-Ruiz et al., 2006; Vives et al., 1999; Yang et al., 1999). Despite the considerable variation observed among CTV isolates, especially in the half of the CTV genome closest to the 5' end (Mawassi et al., 1996), all CTV genomes share a similar pattern of organization and encode 12 open reading frames (ORFs). These ORFs can be translated and processed into at least 17 products (Dawson, 2010), including replication-associated proteins, a homologue of the HSP70 proteins, the two coat proteins and three RNA-silencing suppressors, as well as a few translational products with unknown functions (Lu et al., 2004).

CTV is thought to have originated in the Far East and to have spread to other regions via infected plant propagation material. The virus was then further dispersed throughout most of the world's citrus-growing areas by certain aphid species. There are, however, a few areas, particularly in the Mediterranean basin (Bar-Joseph et al., 1989), in which the disease is not yet widespread. There is an urgent need for control and prevention measures to prevent the spread of CTV into those regions.

One of the major challenges in managing CTV is the considerable diversity of the CTV isolates responsible for some epidemics (Grant

* Corresponding author. Present address: Science and Technology Park of Sicily, Blocco Palma I, Z.I. 95121 Catania, Italy. Tel.: +39 095292731; fax: +39 095292390.
E-mail address: gllicciardello@pstsicilia.it (G. Licciardello).

and Higgins, 1957; Hilf et al., 2005; Kong et al., 2000; Rosner and Bar-Joseph, 1984; Roy et al., 2010; Rubio et al., 2001). Some isolates of CTV can cause considerable losses to scions grafted onto the popular sour orange; whereas similarly sensitive stionic combinations that have been infected by milder CTV isolates often remain free of symptoms for rather long periods (Bar-Joseph et al., 1989). Therefore, for effective management of CTV epidemics, especially during the emerging phase of the disease in an established citrus production area, it is important to rapidly locate and eradicate trees that have been infected by the severe CTV isolates.

The common strategy for managing CTV is based on the eradication of citrus trees regardless of the pathogenic nature of the invading CTV isolates. This strategy has met with considerable resistance from growers and this resistance has often led to the complete abandonment of coordinated attempts to manage the disease. It is, therefore, imperative to be able not only to detect trees that have been recently infected by CTV, but also to determine certain characteristics, such as the potential threat that the newly noticed virus presents to the stionic citrus that are prevalent in the area and its similarity to (or divergence from) earlier invading strains of CTV.

A wide range of methods have been used to differentiate between different CTV isolates, including serology (Permar et al., 1990), molecular hybridization (Rosner and Bar-Joseph, 1984), restriction fragment analyses of amplified CTV cDNA (Gillings et al., 1993), real-time PCR (Ruiz-Ruiz et al., 2009; Roy et al., 2010; Yokomi et al., 2010), genomic sequencing (Karasev et al., 1995) and re-sequencing microarrays (Weng et al., 2007). However, none of these technologies are suitable for the economical and practical categorization of naturally spreading CTV isolates. For epidemiological tests, hundreds and thousands of trees would need to be sampled in cases of disease emergence. Differentiation of CTV strains by analysis of conformational variation of single-stranded DNA sequences (SSCP), although far less informative than the microarray re-sequencing method, can provide useful comparative data regarding the nature of field isolates and also reveal cases of mixed infections involving more than one strain of the virus (Ayllón et al., 1999; D'Urso et al., 2003). Furthermore, it should be noted that, despite considerable recent advances in molecular testing, biological indexing on a set of CTV-sensitive indicator plants remains the only reliable method for the initial assessment of the biological characteristics of a new CTV isolate. This is due to the fact that we still lack sufficiently tested genetic markers for predicting the pathogenicity of CTV isolates that have not been characterized previously. Biological assays are not only costly, but also time-consuming and therefore, less suitable for use in the face of an emerging CTV epidemic, such as the recent case in Sicily (Catara et al., 2008; Catara and Davino, 2006).

The combination of the initial biological characterization of the emerging isolates and their genetic typing by SSCP could allow us to differentiate between different invading CTV virions. However, the SSCP method is time-consuming and labor intensive, mostly due to the work involved in preparing, running and recording non-denaturing polyacrylamide gel analyses. Capillary electrophoresis SSCP (CE-SSCP), which has been used previously to detect mutations (Larsen et al., 2007), construct profiles of bacterial communities (Sen et al., 2008) and categorize isolates of influenza virus (Quinto and Wang, 2004), combines the potential of single-strand conformation analysis with the automation and standardization of electrophoresis run conditions. In this manner, CE-SSCP provides greater resolving power and increased sensitivity and also allows the simultaneous analysis of multiple samples (up to 96 in a single run) with a throughput of 100 samples per day, all without intensive labor (Jespersgaard et al., 2006). Recently, CE-SSCP has also been used to study plant-pathogenic viruses, allowing the quick characterization of CTV isolates (Raspagliesi

et al., 2011) and the analysis of the spatial distribution of a *Plum pox virus* population (Dallot et al., 2008).

This paper describes the further improvement of the CE-SSCP method by applying it specifically to samples that tested positive in ELISA (Bar-Joseph et al., 1979) or dot-blot immunoassays (Cambra et al., 2000). Combining these technologies allows both the rapid location of recent infections and the potential genotyping of the invading CTV virions. This method was applied to plant samples infected with CTV in citrus orchards located in Sicily, in an attempt to distinguish between isolates that induce mild levels of disease symptoms and isolates that induce severe levels of disease for improved disease management. Since the genetic determinants of CTV symptoms are presently unknown, different target regions within p18, p23 and p27 genes were tested in order to determine the best region to use as a molecular marker for pathogenic characters, as well as the clearest and simplest profile for the unequivocal identification of isolates that can induce severe levels of disease symptoms.

The usefulness of the direct use of ELISA eluates or membrane imprints for the molecular characterization of a virus has never been reported. Preliminary results from this work were reported previously at the 18th Conference of the International Organization of Citrus Virologists Congress (Raspagliesi et al., 2010). The proposed method is currently being evaluated by the Italian patent office (Application No. MI2011A000960).

2. Materials and methods

2.1. Source of virus isolates

Eight CTV isolates collected in Sicily were used to test and develop the ELISA/CE-SSCP or dot-blot/CE-SSCP method. Three of the isolates, classified as biotype 4 according to the classification system of Garnsey et al. (2005), were obtained from 25-year-old declining trees of 'Sanguinello' sweet orange grafted onto sour orange, which were referred to as SG29, S24 and S25 (Catara et al., 2010). Isolates 5C and 6D assigned to biotype 4, were collected from *Citrus macrophylla* plants naturally infected by aphids and are reported here for the first time. Of the three isolates that were classified as biotype 1, one was collected from a 5-year-old symptom-less 'Tarocco TDV' sweet orange tree grafted onto 'Troyer' citrange (TDV) (Raspagliesi et al., 2011), one was collected from a symptom-less sour orange seedling naturally infected by aphids (M1) (first description) and one was collected from a symptom-less 'Powell Navel' sweet orange grafted onto 'Troyer' citrange (P60) (first description). Eighteen-month-old sour orange and 'Troyer' citrange seedlings were grafted with the field isolates and maintained in a growth chamber (26 °C – 16 h day/22 °C – 8 h night).

2.2. Biological indexing

Biological characterization was carried out on standard citrus indicator hosts under controlled greenhouse conditions. The eight isolates were graft-inoculated by T-cutting with three bark chips per seedling on three 8-month-old seedlings of sour orange, 'Duncan' grapefruit, Mexican lime and 'Hamlin' sweet orange grafted onto sour orange. A healthy seedling for each indicator was used as control.

2.3. DAS-ELISA and virus release

ELISA was carried out using the Ingezim CTV 2.0 (Ingenasa, Madrid, Spain) commercial kit according to the manufacturer's instructions. Following ELISA, the trapped viral particles were eluted as described by Harju et al. (2005). ELISA plate wells in which there was a positive or a potentially positive reaction were

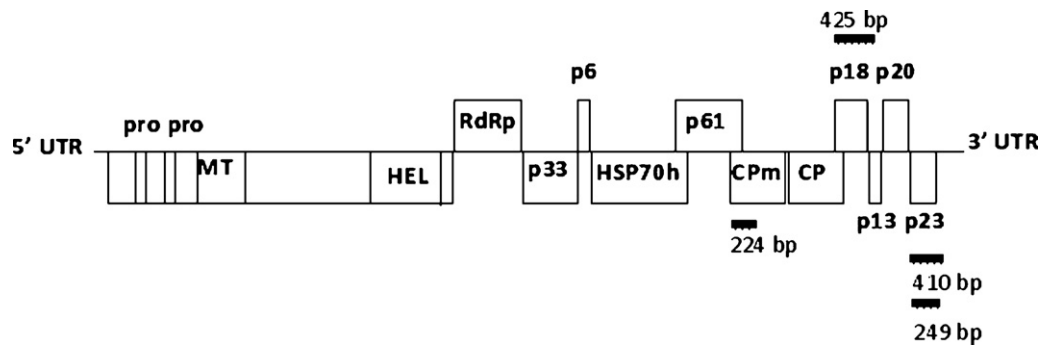


Fig. 1. A diagrammatic presentation of the CTV genome (Karasev et al., 1995) and the positions of the viral regions targeted for amplification in this study. Boxes indicate open reading frames and proteins encoded by different open reading frames are indicated as well. RdRp: RNA-dependent RNA polymerase domain. CPm and CP are the minor and major coat proteins and UTR indicates an untranslated region. Black boxes indicate the positions of target regions used for the CE-SSCP analysis.

washed with phosphate-buffered saline (PBS) solution, tapped dry and immediately processed or stored at -20°C for at least 3–4 weeks and up to 4 months. The wells were then filled with 50 μl of virus-release buffer (VRB) (10 mM Tris–HCl, pH 8.0 with 1.0% (v/v) Triton X-100) and covered to prevent evaporation and the plates were shaken for 5 min at 65°C . After incubation, the extracts were decanted and stored at 5°C , if they were to be processed on the same day, or frozen at -80°C , if they were to be stored for a longer period. Aliquots of these extracts (5 μl) were used for cDNA synthesis, without any further processing.

2.4. Dot-blot immunoassay and trapping release

Dot-blot ELISA (Cambra et al., 2000; OEPP/EPPPO, 2004) was performed with tissue prints on nitrocellulose membranes using a commercial kit (PlantPrint Diagnostics, Valencia, Spain) according to the manufacturer's instructions. Membranes have been stored at room temperature up to four months. Washed membrane spots showing positive reaction, were eluted by placing each spot into an Eppendorf tube containing 100 μl of VRB (10 mM Tris–HCl, pH 8.0 with 1.0% (v/v) Triton X-100). The tubes were incubated at 95°C for 10 min, vortexed and placed on ice, as described by Bertolini et al. (2008). Five- μl aliquots of this extract were used as the templates for one-step RT-PCR assays, without any further processing.

2.5. RNA extraction

Total RNA was extracted from 100-mg samples of fresh, fully expanded citrus leaves previously pulverized with liquid nitrogen using the Trizol reagent (Invitrogen S.r.l., Milan, Italy) according to the manufacturer's instructions.

2.6. Primer design

Three pairs of primers targeting conserved sequences in the p23 and p27 genes of CTV (Fig. 1 and Table 1) were designed using Vector NTI Software (Invitrogen). A multiple alignment of the complete genomic RNA sequences available in databases that correspond to isolates T36 and T30 from Florida (GenBank: U16034 and GenBank: AF260651), VT from Israel (GenBank: U56902), T318A and T385 from Spain (GenBank: DQ151548 and GenBank: Y18420), SY568 from California (GenBank: AF001623), NUagA from Japan (GenBank: AB046398), Qaha from Egypt (GenBank: AY340974) and a Mexican isolate (GenBank: DQ272579) was then carried out.

One PCR product was targeted within the p27 gene and two of different sizes within the p23 gene to test the effect of amplicon length on the ability of the procedure to distinguish between isolates based on the detection of mutations. Primers within the p18 gene (PM44 and PM45) previously described by Sambade et al. (2002), were also used. A schematic diagram of the organization of the CTV genome and the four regions selected for CE-SSCP genotyping is presented in Fig. 1. The primer sequences, annealing temperatures and expected amplicon sizes are presented in Table 1.

2.7. One-step RT-PCR

RT-PCR was performed in a single closed tube containing a final volume of 25 μl . The reaction mix contained 1.6 \times NovaTaq Hot Start Buffer (Novagen, San Diego, CA, USA), 2.5 mM MgCl_2 , 0.4 mM dNTPs, 400 nM of each labelled primer, 0.4 U RNase inhibitor (Applied Biosystems, Foster City, CA, USA), 0.4 U Multiscribe reverse transcriptase (Applied Biosystems), 1.25 U NovaTaq Hot Start DNA polymerase (Novagen) and 5 μl of template RNA from immobilized

Table 1
Primer sets and PCR conditions used in this study.

Gene	Primer set	Sequence	Fluorescent dye	Amplicon size (bp)	Annealing temperature ($^{\circ}\text{C}$)
p18	PM44 ^a PM45 ^a	5'-TTCTATCGGGATGGTGGAGT-3' 5'-GACGAGATTATTACAACGG3'	6-FAM NED	425	56
p27	p27 short FW ^b p27 short RV ^b	5'-GCTCTACGTAAGTATGCTTG-3' 5'-TAACCTTGACGCTAGCTAAC-3'	HEX 6-FAM	224	57
p23	p23 long FW ^b p23 long RV ^b	5'-CTGTGAACCTTTCTGACGAAAG-3' 5'-TCTCGTCTTCTCCCTTCAGC-3'	6-FAM VIC	410	58
p23	p23 long FW p23 short RV	5'-CTGTGAACCTTTCTGACGAAAG-3' 5'-TCTGAGACTGCGTATTGTTGAC-3'	6-FAM HEX	249	58
p23	p23 extFw p23 extRev	5'-GGTTGTATTAACTAATTTAATTCG-3' 5'-AACTTATTCGTCCTCAATCAG-3'		709	56

^a Sambade et al. (2002).

^b Raspagliesi et al. (2010).

Table 2

Biological characterization of disease symptoms induced by eight isolates of *Citrus tristeza virus* on a set of four CTV-indicator plants with three replications.

Isolate	Symptoms ^a			
	Mexican lime	Sour orange	Duncan grapefruit	Sweet orange/sour orange
SG29	LC, VC, SP, Co	SY	SP	Decline
S24	LC, VC, SP, Co	SY	SP	Decline
S25	LC, VC, SP, Co	SY	SP	Decline
6D	LC, VC, SP, Co	SY	SP	Decline
5C	LC, VC, SP, Co	SY	SP	Decline
TDV	LC, VC	–	–	–
M1	LC, VC	–	–	–
P60	LC, VC	–	–	–

^a LC, cupping; VC, vein clearing; SP, stem pitting; Co, vein corking; SY, seedling yellows.

samples or purified RNA. PCR conditions were: 50 °C for 30 min, 95 °C for 7 min, 35 cycles each of 94 °C for 20 s, 56–58 °C (adjusted for each primer set, see Table 2) for 30 s, 72 °C for 40 s, and a final extension at 72 °C for 4 min (Mastercycler EP Gradient Thermocycler, Eppendorf, Milan, Italy).

2.8. CE-SSCP analysis

The analyses were performed using an Applied Biosystems 3130 Genetic Analyzer (Applied Biosystems) equipped with four 36-cm-long capillaries, a window of detection for fluorescent emissions with a spectrum of 480 nm and software to control the temperature, volume and injection time of the samples. Undiluted PCR product (from ELISA/CE-SSCP templates) or PCR product diluted up to 128-fold (in the case of pure template RNA prepared using the conventional CE-SSCP protocol) was mixed with 0.25 µl of GeneScan-500 ROX size standard and 10 µl of formamide Hi-Di (Applied Biosystems). The sample mixture was denatured at 95 °C for 5 min and immediately chilled on ice before being loaded into the instrument. The injection time and voltage were set to 10 s and 3.5 kV and the migration time was set at 1600 s to test different mobility patterns at 24 °C. The non-denaturing polymer mixture that consisted of 5% CAP (POP polymer Conformational Analysis; Applied Biosystems), 10% glycerol and 10× Genetic Analyzer buffer (Applied Biosystems) was used to fill up the capillaries. CE-SSCP profiles were analyzed using GeneMapper Software, version 4 (Applied Biosystems). Variations in run-to-run time were compensated by normalizing each run with the internal size standard according to the rate of fragment migration and depending on conformation. For each run, standard fragments surrounding the sample fragments were used to estimate size of the sample strands, expressed as migration time data points. Differences between the migration times associated with the peaks for the different samples were expressed as standard deviations. Three to six replicates of each sample and standard deviations were calculated to evaluate the variability within and between runs.

2.9. Molecular cloning and nucleotide sequence analysis of the p23 gene

The full-length p23 genes of the SG29, 5C, P60, 6D and M1 CTV isolates were sequenced after cloning. Viral targets were amplified by one-step RT-PCR with external primers p23 extFw and p23 extRw (Table 1) and then purified using the QIAquick gel extraction kit (Qiagen, Milan, Italy) according to the manufacturer's instructions, ligated into the pTZ57R/T vector (Fermentas Inc., Maryland, USA) using the InsTAclone PCR cloning kit (Fermentas) and transformed into competent *Escherichia coli* DH5α cells as described by Sambrook and Russell (2001).

Several white colonies suspected of harboring the recombinant plasmid were selected on the surface of Luria–Bertani (LB)

agar plates treated with 40 µl X-gal (5-bromo-4-chloro-3-indolyl-β-D-galactoside) (Sigma Aldrich Chemical Company, Poole, United Kingdom) and ampicillin (50 mg/L). Plasmid was extracted from these cultures by boiling the material for 10 min in a water bath. PCR amplicons of the long p23 fragment that were derived from the ampicillin-resistant colonies were subjected to CE-SSCP, in order to construct profiles and limit the number of clones to be sequenced. Mini-preps of DNA from clones were purified using the QIAprep kit (Qiagen). The presence of the expected CTV gene product in each of these clones was confirmed by direct sequencing of the entire clone with M13 universal primers using the Dye Terminator Cycling Sequencing (DTCS) Quick Start kit (P/N 608120) provided by Beckman Coulter (Milan, Italy). Cycle-sequencing conditions were 30 cycles of 96 °C for 20 s, 50 °C for 20 s and 60 °C for 4 min. The reactions were purified by ethanol precipitation, dried, resuspended in 40 µl of the Sample Loading Solution (provided in the kit) and then run in a CEQ 8000 Genetic Analyzer System (Beckman Coulter).

The p23 gene nucleotide sequences were deposited in the GenBank database under the accession codes JN384021–JN384024. Partial sequences of the p23 genes of S24 (GenBank: EU487601), S25 (GenBank: EU483657) and TDV (GenBank: EU487603) (Catara et al., 2010) were also examined. Multiple sequence alignments were performed using the BioEdit 7.0.9 program.

3. Results

3.1. ELISA and biological characterization of CTV isolates

As part of the development of the sequential ELISA/CE-SSCP protocol and its application as a combined method for CTV screening and isolate partial genotyping, plant material from Sicilian citrus orchards was collected and subjected to DAS-ELISA for serological detection of CTV infections. The host reactions of the selected isolates were evaluated on CTV-indicator plants and the results of this evaluation suggest that these isolates can be grouped into two main categories (Table 2). One group, consisting of SG29, S24, S25, 6D and 5C, induced leaf cupping, vein clearing, stem pitting and vein corking on Mexican lime; seedling yellow on sour orange; stem pitting on 'Duncan' grapefruit and decline without stem pitting on 'Hamlin' sweet orange grafted onto sour orange. According to the biotype classification described by Garnsey et al. (2005), these isolates can be classified as biotype 4, a group that includes CTV isolates known to induce severe disease symptoms. Isolates TDV, M1 and P60 induced mild symptoms on Mexican lime and no symptoms on sour orange, Duncan grapefruit or sweet orange grafted onto sour orange and were, therefore, classified as biotype 1 (Table 2).

3.2. Comparative analysis of CE-SSCP runs using RNA extracts and ELISA plate eluates

RNA from eight CTV isolates was recovered from the positively reacting ELISA wells and characterized in a sequential process by direct amplification using fluorescent primers and CE-SSCP. The

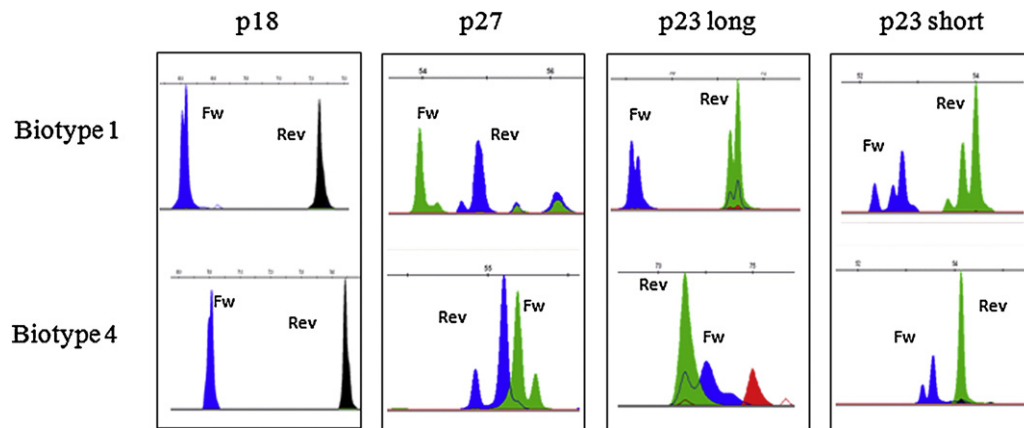


Fig. 2. Representative electrophoretic profiles of CTV isolates of biotypes 1 and 4 that were collected in Sicily and subjected to sequential ELISA/CE-SSCP (p18 gene product) and dot-blot/CE-SSCP (p27, p23 long and p23 short gene products) analyses. Peaks correspond to the fluorescent labels of the single-stranded DNA fragments (forward, Fw and reverse, Rev) detected by the automated sequencer using Genescan 500 ROX as a size standard for peak pattern alignment. Given profiles are representative of at least 3 replications runs on 3 different experiments. (For interpretation of the references to color in this figure legend, the reader is referred to the web version of this article.)

mobility values and peak profiles of forward and reverse strands of the partial p18 gene (Fig. 2) were used for the initial characterization of the CTV isolates.

Migration of sample peaks was calculated and normalized relative to the internal size standard, in order to eliminate the effect of any capillary-to-capillary or run-to-run variability. The peak profiles of forward and reverse strand conformers were different and could be distinguished by the different colors of the fluorophore. The CE-SSCP conformation peaks were clear and reproducible and the profiles showed at least two different migration patterns, allowing the differentiation of the tested CTV isolates into two defined groups, which correlated with the mild and the severe reactions that we observed on the host plants in the whole-plant assay (Table 2). The profiles of the p18 gene fragments from isolates TDV, M1 and P60, each had two peaks and mobility values (sizes) of about 70.5 and 73.8 for the forward and reverse primers, respectively (Table 3). The migration pattern of the isolates that induced severe disease symptoms, SG29, S24, S25 (collected from three trees located in close proximity to one another in a single orchard), 6D and 5C, had shifted profiles with mobility peaks with “size” values of about 72.3 and 75.9 for the forward and reverse strands, respectively.

To validate this new protocol, the migration patterns obtained using the sequential ELISA/CE-SSCP protocol were compared with profiles obtained from the analysis of RNA extracted directly from the corresponding leaves. The data point and profile obtained using the two procedures were essentially similar or highly correlated

with one another and were clear and reproducible, indicating the robustness of the new method (Table 3).

When the sequential ELISA/CE-SSCP protocol was applied to samples that, after DAS-ELISA, showed an optical density near or below the cut-off value ($OD < 0.200$), we were still able to obtain clear migration profiles, suggesting that the sensitivity of ELISA detection was considerably increased by the PCR amplification process applied directly to the microtiter plate (data not shown). Reproducible results have also been obtained for samples from microtiter plates stored at -20°C for at least 3–4 weeks and up to 4 months.

3.3. Analysis of CE-SSCP profiles using dot-blot immunoassay eluates

For testing the possible sequential analysis of plant samples following dot-blot immunoassays, the alignment of 20 full-length CTV genomes was used to design three sets of primers that amplified two regions of p23 gene with different amplicon sizes of 249 bp and 410 bp and an additional primer set that resulted in a 224 bp amplicon of the p27 minor coat protein (CPm) gene. The migration profiles of single strands obtained when membrane spot eluates were used as templates for PCR amplification were clear and reproducible (Fig. 2 and Table 4) and were comparable with those obtained from total RNA templates (data not shown). Each strand could be distinguished by the different colors of the fluorophores. For all of the CTV genomic regions tested, different profiles were

Table 3

Peak positions of forward and reverse single-stranded p18 cDNA molecules determined by CE-SSCP analysis of RNA extracts or ELISA plate eluates from eight Sicilian CTV isolates of two different biotypes.

CTV isolate	Biotype ^a	Peak relative migration			
		ELISA/CE-SSCP		RNA	
		FW ^b	REV ^c	FW ^b	REV ^c
SG29	4	72.52 ± 0.08	75.81 ± 0.17	72.43 ± 0.18	75.78 ± 0.25
S24	4	72.47 ± 0.12	75.69 ± 0.23	72.44 ± 0.32	75.76 ± 0.07
S25	4	72.59 ± 0.38	75.77 ± 0.09	72.39 ± 0.27	75.78 ± 0.22
6D	4	72.31 ± 0.04	75.83 ± 0.30	72.77 ± 0.05	75.39 ± 0.07
5C	4	72.54 ± 0.03	75.74 ± 0.05	72.68 ± 0.12	75.47 ± 0.23
TDV	1	70.35 ± 0.21	73.91 ± 0.18	70.27 ± 0.15	73.85 ± 0.21
M1	1	70.48 ± 0.07	73.32 ± 0.01	70.65 ± 0.12	73.58 ± 0.03
P60	1	70.54 ± 0.12	74.02 ± 0.14	70.41 ± 0.04	73.29 ± 0.01

^a According to Garnsey et al., 2005.

^b FW: forward.

^c REV: reverse.

Table 4
Peak positions of forward and reverse single-stranded cDNA molecules of p23 and p27 gene products determined by CE-SSCP performed using material obtained from eluates of dot blots of eight immuno-positive CTV isolates collected in Sicily.

Isolate	Biotype ^a	Peak relative migration					
		p23 long (410 bp)		p23 short (249 bp)		p27 (224 bp)	
		FW ^b	REV ^c	FW ^b	REV ^c	FW ^b	REV ^c
SG29	4	72.14 ± 0.12	72.14 ± 0.32	54.35 ± 0.70	55.11 ± 0.92	55.17 ± 0.25	54.64 ± 0.21
		72.51 ± 0.02		54.56 ± 0.32		55.39 ± 0.11	55.00 ± 0.36
S24	4	72.81 ± 0.01	72.81 ± 0.02	53.33 ± 0.09	54.14 ± 0.22	55.32 ± 0.05	54.80 ± 0.12
		73.21 ± 0.30		53.56 ± 0.01		55.50 ± 0.14	55.10 ± 0.31
S25	4	72.88 ± 0.23	72.78 ± 0.44	53.89 ± 0.03	54.51 ± 0.02	55.28 ± 0.22	54.78 ± 0.20
		73.24 ± 0.06		53.99 ± 0.12		55.48 ± 0.16	55.06 ± 0.40
6D	4	72.78 ± 0.07	72.28 ± 0.12	54.37 ± 0.37	55.13 ± 0.11	55.30 ± 0.43	54.69 ± 0.31
		73.19 ± 0.05		54.58 ± 0.54		55.51 ± 0.33	55.10 ± 0.34
5C	4	72.95 ± 0.32	73.06 ± 0.85	53.10 ± 0.12	54.54 ± 0.98	55.36 ± 0.08	54.83 ± 0.23
		73.30 ± 0.64		53.35 ± 0.09		55.58 ± 0.26	55.16 ± 0.21
TDV	1	69.21 ± 0.01	71.29 ± 0.04	52.56 ± 0.66	53.99 ± 0.07	53.82 ± 0.08	54.35 ± 0.02
			71.46 ± 0.21	52.98 ± 0.43	54.08 ± 0.06	54.09 ± 0.11	54.65 ± 0.09
				53.06 ± 0.01	54.29 ± 0.11		
P60	1	70.05 ± 0.21	72.25 ± 0.02	52.26 ± 0.54	53.51 ± 0.05	53.91 ± 0.04	54.49 ± 0.06
			72.44 ± 0.32	52.58 ± 0.32	53.77 ± 0.23	54.18 ± 0.16	54.79 ± 0.03
				52.73 ± 0.03	53.99 ± 0.54		
M1	1	68.34 ± 0.12	70.49 ± 0.07	53.33 ± 0.32	54.48 ± 0.39	54.17 ± 0.10	54.84 ± 0.02
			70.67 ± 0.45	53.62 ± 0.14	54.71 ± 0.12	54.45 ± 0.16	55.15 ± 0.11
				53.77 ± 0.62	54.91 ± 0.62		

^a According to Garnsey et al., 2005.

^b FW: forward.

^c REV: reverse.

obtained for isolates belonging to biotypes 1 and 4, demonstrating the usefulness of this method for categorizing CTV isolates. The analysis of the p23 gene revealed that both the long (410 bp) and short (249 bp) PCR products can be used to distinguish between CTV isolates in the same two groups. The p23 long fragment profiles obtained from isolates that induce mild disease showed two distinct peaks, each with two spikes for the forward (blue) and reverse (green) strands (Fig. 2). Clearly different were the profiles obtained for the isolates that induced severe disease, which showed two peaks for forward strand (blue) and one peak for reverse strand (green) that overlapped the first blue peak (Fig. 2). Sequence alignment revealed the presence of 42 nucleotide mutations between the two groups of isolates (Fig. 3).

The profiles obtained for the p23 short PCR product, which was internal to the long one so as to restrict detectable mutations and allow better discrimination among isolates of the same group, were clearly different for the different isolates. Within this PCR product, 29 mutations were detected between the two groups of isolates. The three isolates that induce mild disease, TDV, M1 and P60, all had similar strand conformers that consisted of at least 6 peaks, three peaks for the forward strand in the first part of the electropherogram and three for the reverse strand, which migrates more slowly. Only two punctiform mutations, which do not have much influence on secondary structure, were detected. In contrast, the profiles of the severe isolates consisted of three peaks, two for the forward strand and one for the reverse, and were identical for all of the tested isolates, as confirmed by 100% nucleotide sequence homology and the fact that no mutations were detected (Fig. 3).

Based on the electrophoretic mobility shifts of the p27 gene single-strand conformations (224 bp), the isolates that induce mild symptoms, TDV, M1 and P60 mild, each had a four-peak profile consisting of one main peak for the forward strand (green) with a little hump on the right and one main peak for the reverse one (blue) with a little hump on the left. A different profile was noted for the isolates that induce severe disease, which could be differentiated by the inverted positions of the single-stranded conformers.

In fact, the profile consisted of a group of four peaks, two peaks for the reverse strand (green) in the first part, which partially overlap the two peaks of the forward strand (blue) (Fig. 2). This relative migration of the two strands was confirmed in 30 subsequent tests run on isolates that induce severe disease symptoms.

4. Discussion

Characterization of isolates of CTV and other viruses is of considerable importance for disease control, especially as a tool to prioritize and select trees to be rapidly eliminated during the emerging stages of an epidemic. Tristeza decline is a serious threat to the citrus industry, due to the dispersal of severe isolates that cause stunting and stem pitting in grapefruit or sweet orange, regardless of the rootstock used. This fact necessitates the control of the disease through different measures involving efficient procedures to identify potentially dangerous isolates. Although several serological and molecular markers have been used to characterize isolates (Hilf et al., 2005; Sambade et al., 2003), the variability in pathogenicity among isolates precludes the association of specific symptoms with a specific genotype and the presence of mixed populations on the same plant increases the difficulty of this process.

The method described in this paper is designed to assess rapidly the disease situation in those areas in which severe CTV isolates are present. Although a similar procedure involving tissue-print ELISA and real-time PCR has been proposed for direct virus quantification (Bertolini et al., 2008), this is the first report of an immunological test combined with a partial genotypic analysis for the rapid characterization of CTV targets in plant tissues based on single-strand conformation analysis.

Conventional SSCP analysis has been improved further by capillary electrophoresis and its combination with the ELISA and/or dot-blot immunoassays that are commonly used to detect CTV (Bar-Joseph et al., 1979; Cambra et al., 2000). Combining these procedures, enables both to locate newly infected trees and

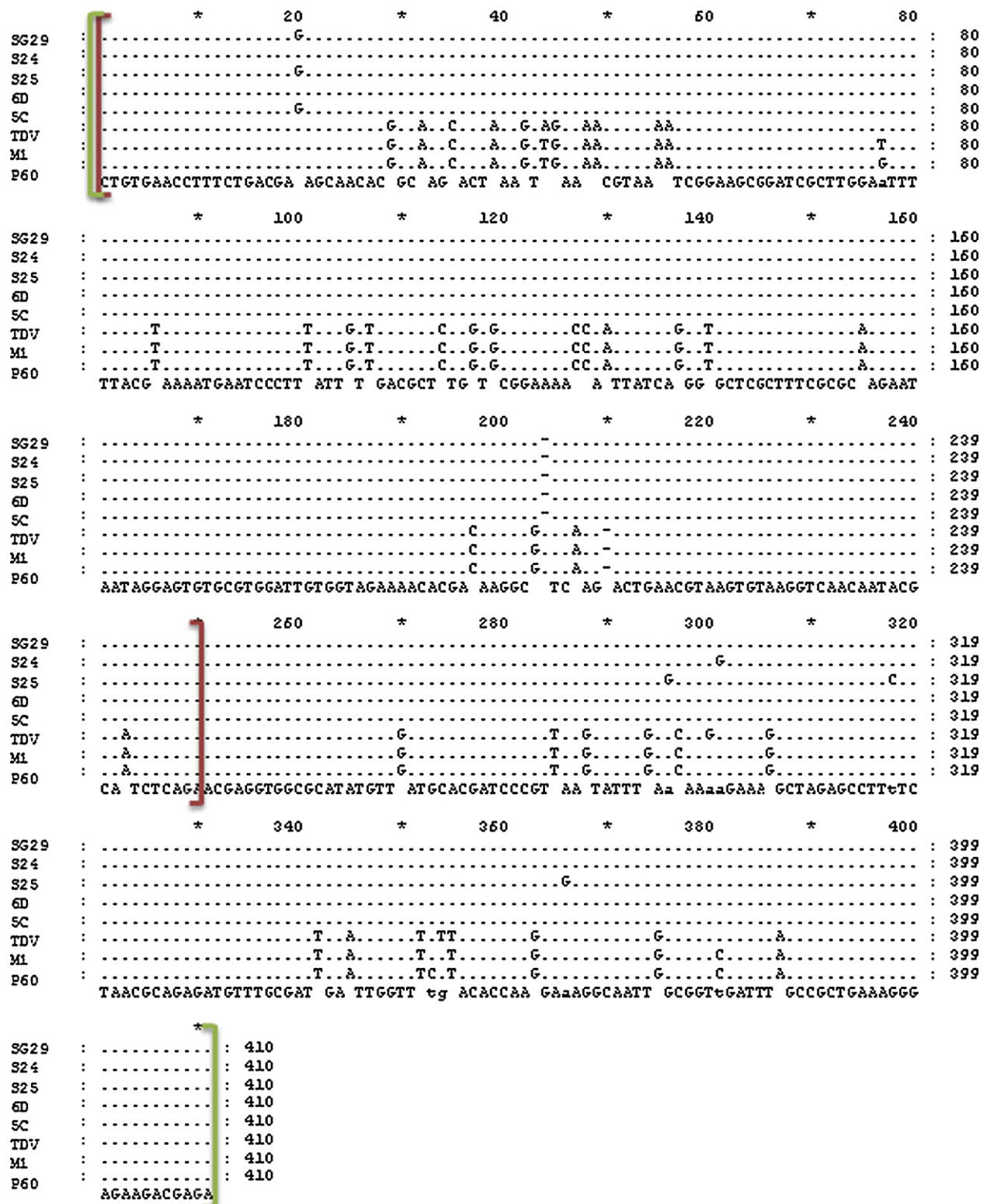


Fig. 3. Alignment of nucleotide sequences of CTV isolates classified as biotype 4 (SG29, S24, S25, 6D, and 5C) and biotype 1 (TDV, M1, and P60). Green brackets (delimiting the entire fragment) refer to the p23 long PCR fragment. Red brackets (inside the fragment) refer to the p23 short PCR product. For each position, identical residues are indicated by dots. (For interpretation of the references to color in this figure legend, the reader is referred to the web version of this article.)

analyze immediately the genotype of the infecting virus, allowing the rapid identification of trees infected with strains of the virus that have SSCP profiles associated with CTV strains known to induce severe disease symptoms, so that these trees can be targeted for elimination.

This method of predicting the pathogenicity characteristics of CTV isolates has been successfully used to distinguish between the two biotypes most commonly found in Sicilian groves. The results concerning the p23 and p27 genes that are presented here clearly demonstrate that isolates belonging to biotype 4, which cause

severe disease symptoms on sour orange and grapefruit and decline of sweet orange, can be distinguished from biotype 1 isolates, which induce only mild disease symptoms. Although additional biological tests will be necessary to determine the pathogenic nature of CTV isolates, with new SSCP migration patterns, nevertheless, the sequential immuno-detection and CE-SSCP is expected to provide us with a fast warning system to reliably predict the potential threat presented by emerging isolates. Indeed work in progress is aimed to screen and extend this procedure to all CTV biotypes, currently present in Italy and to provide a useful and complete tool for virus discrimination. Other highly variable genomic regions may be also tested and considered. Furthermore such typing is helpful for monitoring the spatial patterns and genetic structure of CTV populations and for following the appearance and spread of resistance-breaking CTV isolates, such as those recently reported in New Zealand (Harper et al., 2010).

SSCP analyses of different regions of genomic RNA have been widely used in recent years to characterize the structures of populations of different strains of CTV (Ayllón et al., 1999; D'Urso et al., 2003). However, the greater resolving power of CE-SSCP, due to capillary length and polymer properties, provides considerable improvement in terms of both the possible scale of operation and reproducibility.

This method may be used widely for CTV cross-protection studies (Bederski et al., 2005; Broadbent et al., 1991; Costa and Müller, 1980; Sambade et al., 2002), empowering the capability of SSCP to monitor temporal evolution of the CTV population in doubly inoculated plants, according to the migration and intensity of fluorescence of distinct peaks. The recent report of Folimonova et al. (2010) clearly indicated that effective cross-protection is only expected in cases in which the invading (challenging), naturally spreading CTV strain is met by a similar mild genotype. In addition, due to the suitability of the immunoblot tests for sampling field trees and nursery plants, the sequential combination of immunoblot tests with automated CE-SSCP is expected to facilitate epidemiological analyses considerably and to allow improved large-scale screening for CTV and other viruses at a reduced cost and with increased precision and speed. The encapsidated RNA samples from immobilized virions are stable on membranes for a long period (several months), allowing the samples to be easily transferred to diagnostic laboratories. The most significant advantages of the method described in this paper over the use of conventional ELISA or dot-blot eluates are the time and labor savings this method provides by eliminating the need for any re-sampling, additional extract preparation or RNA purification. The extraction method described takes around 10 min per individual sample. This is in contrast to the Trizol extraction method, in which the analysis of each sample requires at least 2 h, including the grinding of the material in liquid nitrogen.

In comparison with conventional SSCP, the use of capillary electrophoresis allows us to avoid the need for an acrylamide gel and due to the automatic acquisition and storage of data, greatly improves the information that can be potentially obtained from the analysis of single-strand polymorphisms. In particular, the possibility of differentiating between the conformers of each single strand based on curve shape and their relative position in the profile, thanks to the use of different fluorophores, contributes very well to the clear and simple discrimination of isolates. This increases the cost of the process (since the primers are expensive), but also makes it easier to read the electropherograms and allows for clearer resolution in situations involving overlapping or inverted peaks. The inverted position of the reverse strand relative to the forward one, evident in the profile of the p27 gene product and p23 long fragment, appears to be distinctive of CTV isolates that induce severe disease symptoms and is easy to detect. Moreover, in cases in which a mixed population is present in the same

plant tissue, the high sensitivity of capillary electrophoresis facilitates the unequivocal determination of the single virus component and the detection of minor variants. Analysis of PCR products ranging from 200 to 300 bp in size increases the sensitivity and clarity of the conformers, allowing us to detect crucial mutations more easily than 400-bp products and to differentiate easily between individual variants.

Acknowledgements

This work was supported by the IT-Citrus Genomics project (PON01 01623) funded by the Italian MIUR (Ministero dell'Istruzione, dell'Università e della Ricerca) PON 2007–2013 and UE. The authors would like to thank A. Lombardo for contributing to the design of the primers and A. Bertuccio, S. Fassari and A. Santonocito of the Laboratory for Phytosanitary Diagnoses and Biotechnology, Science and Technology Park of Sicily, for providing samples used in this research and for help collecting and testing samples.

References

- Albiach-Martí, M.R., Mawassi, M., Gowda, S., Satyanarayana, T., Hilf, M.E., Shanker, S., Almira, E.C., Vives, M.C., López, C., Guerri, J., Flores, R., Moreno, P., Garnsey, S.M., Dawson, W.O., 2000. Sequences of *Citrus tristeza virus* separated in time and space are essentially identical. *J. Virol.* 74, 6856–6865.
- Ayllón, M.A., Rubio, L., Moya, A., Guerri, J., Moreno, P., 1999. The haplotype distribution of two genes of *Citrus tristeza virus* is altered after host change or aphid transmission. *Virology* 255, 32–39.
- Bar-Joseph, M., Dawson, W.O., 2008. *Citrus tristeza virus*. In: Mahy, B.W.J., Regenmortel, M.H.V. (Eds.), *Encyclopedia of Plant and Fungal Viruses*. Elsevier, Oxford, UK, pp. 520–525.
- Bar-Joseph, M., Garnsey, S.M., Gonsalves, D., Moscovitz, M., Purcifull, D.E., Clark, M.F., Loebenstein, G., 1979. The use of enzyme-linked immunosorbent assay for detection of *Citrus tristeza virus*. *Phytopathology* 69, 190–194.
- Bar-Joseph, M., Marcus, R., Lee, R.F., 1989. The continuous challenge of *Citrus tristeza virus* control. *Annu. Rev. Phytopathol.* 27, 291–316.
- Bederski, K., Roistacher, C.N., Müller, G.W., 2005. Cross protection against the severe *Citrus tristeza virus*: stem pitting in Peru. In: Proc. 16th Conf. Int. Org. Citrus Virol., IOCV, Riverside, CA, pp. 117–126.
- Bertolini, E., Moreno, A., Copote, N., Olmos, A., De Luis, A., Vidal, E., Pérez-Panadés, J., Cambra, M., 2008. Quantitative detection of *Citrus tristeza virus* in plant tissues and single aphid by real-time RT-PCR. *J. Plant Pathol.* 120, 177–188.
- Broadbent, P., Bevington, K.B., Coote, B.G., 1991. Control of stem pitting of grapefruit in Australia by mild strain cross protection. In: Proc. 11th Conf. Int. Org. Citrus Virol., IOCV, Riverside, CA, pp. 64–70.
- Cambra, M., Gorris, M.T., Román, M.P., Terrada, E., Garnsey, S.M., Camarasa, E., Olmos, A., Colomer, M., 2000. Routine detection of *Citrus tristeza virus* by direct immunoprinting – ELISA method using specific monoclonal and recombinant antibodies. In: Proc. 14th Conf. Int. Org. Citrus Virol., IOCV, Riverside, CA, pp. 34–41.
- Catara, A., Barbagallo, S., Saponari, M., 2008. Il caso “tristeza” degli agrumi. *I Georgofili-Quaderni* 6, 123–138.
- Catara, A., Davino, M., 2006. Il virus della tristeza degli agrumi in Sicilia. *Frutticoltura* 1, 18–23.
- Catara, A., Lombardo, A., Nobile, G., Rizza, S., 2010. Characterization of additional *Citrus tristeza virus* isolates in a highly infected citrus area of Sicily. In: Proc. 17th Conf. Int. Org. Citrus Virol., IOCV, Riverside, CA, pp. 80–83.
- Costa, A.S., Müller, G.W., 1980. Tristeza control by cross-protection: US–Brazil cooperative success. *Plant Dis.* 64, 538–541.
- Dallot, S., Boeglin, M., Labonne, G., 2008. Spatial pattern and genetic structure of PPV-M in a delimited area of stone fruit orchards in southern France. *Acta Hort.* 781, 235–242.
- Dawson, W.O., 2010. Molecular genetics of *Citrus tristeza virus*. In: Karasev, A.V., Hilf, M.E. (Eds.), *Citrus tristeza virus Complex and Tristeza Diseases*. APS Press, The American Phytopathological Society, St. Paul, MN, pp. 53–72.
- D'Urso, F., Sambade, A., Moya, A., Guerri, J., Moreno, P., 2003. Variation of haplotype distributions of two genomic regions of *Citrus tristeza virus* populations from eastern Spain. *Mol. Ecol.* 12, 517–526.
- Febres, V.J., Ashoulin, L., Mawassi, M., Frank, A., Bar-Joseph, M., Manjunath, K.L., Lee, R.F., Niblett, C.L., 1996. The p27 protein is present at one end of *Citrus tristeza virus* particles. *Phytopathology* 86, 1331–1335.
- Folimonova, S.Y., Robertson, C.J., Shilts, T., Folimonov, A.S., Hilf, M.E., Garnsey, S.M., Dawson, W.O., 2010. Infection with strains of *Citrus tristeza virus* does not exclude superinfection by other strains of the virus. *J. Virol.* 84, 1314–1325.
- Garnsey, S.M., Civerolo, E.L., Gumpf, D.J., Paul, C., Hilf, M.E., Lee, R.F., Bransky, R.H., Yokomi, R.K., Hartung, J.S., 2005. Biological characterization of an international collection of *Citrus tristeza virus* (CTV) isolates. In: Proc. 16th Conf. Int. Org. Citrus Virol., IOCV Riverside, CA, pp. 75–93.

- Gillings, M., Broadbent, P., Indsto, J., Lee, R., 1993. Characterization of isolates and strains of *Citrus tristeza closterovirus* using restriction analysis of the coat protein gene amplified by the polymerase chain reaction. *J. Virol. Methods* 44, 305–317.
- Grant, T.J., Higgins, R.P., 1957. Occurrence of mixtures of tristeza virus strains in citrus. *Phytopathology* 47, 272–276.
- Harju, V.A., Skelton, A., Clover, G.R.G., Ratti, C., Boonham, N., Henry, C.M., Mumford, R.A., 2005. The use of real-time RT-PCR TaqMan (R) and post-ELISA virus release for the detection of beet necrotic yellow vein virus types containing RNA 5 and its comparison with conventional RT-PCR. *J. Virol. Methods* 123, 73–80.
- Harper, S.J., Dawson, T.E., Pearson, M.N., 2010. Isolates of *Citrus tristeza virus* that overcome *Poncirus trifoliata* resistance comprise a novel strain. *Arch. Virol.* 155, 471–480.
- Hilf, M.E., Mavrodieva, V.A., Garnsey, S.M., 2005. Genetic marker analysis of a global collection of isolates of *Citrus tristeza virus*: characterization and distribution of CTV genotypes and association with symptoms. *Phytopathology* 95, 909–917.
- Jespersgaard, C., Larsen, L.A., Baba, S., Kukita, Y., Tahira, T., Christiansen, M., Vuust, J., Hayashi, K., Andersen, P.S., 2006. Optimization of capillary array electrophoresis single-strand conformation polymorphism analysis for routine molecular diagnostics. *Electrophoresis* 27, 3816–3822.
- Karasev, A.V., Boyko, V.P., Gowda, S., Nikolaeva, O.V., Hilf, M.E., Koonin, E.V., Niblett, C.L., Cline, K., Gumpf, D.J., Lee, R.F., Garnsey, S.M., Dawson, W.O., 1995. Complete sequence of the *Citrus tristeza virus* RNA genome. *Virology* 208, 511–520.
- Karasev, A.V., Hilf, M.E., 2010. *Citrus tristeza virus* Complex and Tristeza Diseases. APS Press, The American Phytopathological Society, St. Paul, MN.
- Kong, P., Rubio, L., Polek, M., Falk, B.W., 2000. Population structure and genetic diversity within California *Citrus tristeza virus* (CTV) field isolates. *Virus Genes* 21, 139–145.
- Larsen, L.A., Jespersgaard, C., Andersen, P.S., 2007. Single-strand conformation polymorphism analysis using capillary electrophoresis for large-scale mutation detection. *Nat. Protoc.* 2, 1458–1466.
- Lu, R., Folimonov, A., Shintaku, M., Li, W.X., Falk, B.W., Dawson, W.O., Ding, S.W., 2004. Three distinct suppressors of RNA silencing encoded by a 20-kb viral RNA genome. *Proc. Natl. Acad. Sci. U.S.A.* 101, 15742–15747.
- Mawassi, M., Mietkiewska, E., Gofman, R., Yang, G., Bar-Joseph, M., 1996. Unusual sequence relationships between two isolates of *Citrus tristeza virus*. *J. Gen. Virol.* 77, 2359–2364.
- Moreno, P., Ambrós, S., Albiach-Martí, M.R., Guerri, J., Peña, L., 2008. *Citrus tristeza virus*: a pathogen that changed the course of the citrus industry. *Mol. Plant Pathol.* 9, 251–268.
- OEPP/EPPPO, 2004. Diagnostic protocols for regulated pests/Protocoles de diagnostic pour les organismes réglementés – *Citrus tristeza closterovirus*. OEPP/EPPPO Bull. 34, 155–157.
- Permar, T.A., Garnsey, S.M., Gumpf, D.J., Lee, R.F., 1990. A monoclonal antibody which discriminates strains of *Citrus tristeza virus*. *Phytopathology* 80, 224–228.
- Quinto, J.D., Wang, C.K., 2004. A high-throughput single-stranded conformation polymorphism assay for detection, subtyping and genotyping of influenza viruses. *Proc. Int. Congr. Ser.* 1263, 653–657.
- Raspagliesi, D., Licciardello, G., Lombardo, A., Rizza, S., Bar-Joseph, M., Catara, A., 2010. Rapid detection and characterization of *Citrus tristeza virus* isolates by sequential ELISA/CE-SSCP. In: *Proc. 18th Conf. Int. Org. Citrus Virol. IOCV*, Riverside, CA, in press.
- Raspagliesi, D., Licciardello, G., Rizza, S., Lombardo, A., Catara, A., 2011. Quick characterization of *Citrus tristeza virus* isolates by capillary electrophoresis-single-strand conformation polymorphism. *Acta Hort.* 892, 183–188.
- Rosner, A., Bar-Joseph, M., 1984. Diversity of *Citrus tristeza virus* strains indicated by hybridization with cloned cDNA sequences. *Virology* 139, 189–193.
- Roy, A., Ananthakrishnan, G., Hartung, J.S., Brlansky, R.H., 2010. Development and application of a multiplex reverse-transcription polymerase chain reaction assay for screening a global collection of *Citrus tristeza virus* isolates. *Phytopathology* 100, 1077–1088.
- Rubio, L., Ayllón, M.A., Kong, P., Fernández, A., Polek, M.L., Guerri, J., Moreno, P., Falk, B.W., 2001. Genetic variation of *Citrus tristeza virus* isolates from California and Spain: evidence for mixed infections and recombination. *J. Virol.* 75, 8054–8062.
- Ruiz-Ruiz, S., Moreno, P., Guerri, J., Ambrós, S., 2006. The complete nucleotide sequence of a severe stem pitting isolate of *Citrus tristeza virus* from Spain: comparison with isolates from different origins. *Arch. Virol.* 151, 387–398.
- Ruiz-Ruiz, S., Moreno, P., Guerri, J., Ambrós, S., 2009. Discrimination between mild and severe *Citrus tristeza virus* isolates with a rapid and highly specific real-time reverse transcription-polymerase chain reaction method using TaqMan LNA probes. *Phytopathology* 99, 307–315.
- Sambade, A., López, C., Rubio, L., Flores, R., Guerri, J., Moreno, P., 2003. Polymorphism of a specific region in gene p23 of *Citrus tristeza virus* allows discrimination between mild and severe isolates. *Arch. Virol.* 148, 2325–2340.
- Sambade, A., Rubio, L., Garnsey, S.M., Costa, N., Müller, G.W., Peyrou, M., Guerri, J., Moreno, P., 2002. Comparison of viral RNA populations of pathogenically distinct isolates of *Citrus tristeza virus*: application to monitoring cross-protection. *Plant Pathol.* 51, 257–265.
- Sambrook, J., Russell, D., 2001. *Molecular Cloning: A Laboratory Manual*, 3rd ed. Cold Spring Harbor Laboratory Press, Cold Spring Harbor, NY.
- Sen, B., Hamelin, J., Bru-Adan, V., Godon, J.-J., Chandra, T.S., 2008. Structural divergence of bacterial communities from functionally similar laboratory-scale vermicomposts assessed by PCR-CE-SSCP. *J. Appl. Microbiol.* 105, 2123–2132.
- Vives, M.C., Rubio, L., López, C., Navas-Castillo, J., Albiach-Martí, M.R., Dawson, W.O., Guerri, J., Flores, R., Moreno, P., 1999. The complete genome sequence of the major component of a mild *Citrus tristeza virus* isolate. *J. Gen. Virol.* 80, 811–816.
- Weng, Z., Barthelson, R., Gowda, S., Hilf, M.E., Dawson, W.O., Galbraith, D.W., Xiong, Z., 2007. Persistent infection and promiscuous recombination of multiple genotypes of an RNA virus within a single host generate extensive diversity. *PLoS One* 2, e917.
- Yang, N., Mathews, D.M., Dodds, J.A., Mirkov, T.E., 1999. Molecular characterization of an isolate of *Citrus tristeza virus* that causes severe symptoms in sweet orange. *Virus Genes* 19, 131–142.
- Yokomi, R.K., Saponari, M., Sieburth, P.J., 2010. Rapid differentiation and identification of potential severe strains of *Citrus tristeza virus* by real-time reverse transcription-polymerase chain reaction assays. *Phytopathology* 100, 319–327.